Gravitational lenses and cosmological evolution

J. A. Peacock *Royal Observatory, Blackford Hill, Edinburgh EH9 3HJ*

Summary. The effect of gravitational lensing on the apparent cosmological evolution of extragalactic radio sources is investigated. Models for a lens population consisting of galaxies and clusters of galaxies are constructed and used to calculate the distribution of amplification factors caused by lensing. Although many objects at high redshifts are predicted to have flux densities altered by 10–20 per cent relative to a homogeneous universe, flux conservation implies that de-amplification is as common as amplification. The effects on cosmological evolution as inferred from source counts and redshift data are thus relatively small; the slope of the counts is not large enough for intrinsically rare lensing events of high amplitude to corrupt observed samples. Lensing effects may be of greater importance for optically selected quasars, where lenses of mass as low as $\sim 10^{-4} M_\odot$ can cause large amplifications.

1 Introduction

The cosmological evolution of quasars and active galaxies is potentially one of the most important tools for studying the Universe at early epochs. Redshift and number-count data may be combined to yield the time-dependence of the luminosity function, which relates to the creation and evolution of individual objects. Evolutionary studies have been carried out at both radio and optical frequencies, with broadly similar conclusions: the most powerful objects in a given waveband exhibit large changes in their comoving densities, which were typically greater at a redshift of 1 than at present by factors of $\sim 10^3$–10^4. The data available in the radio waveband are more extensive than in the optical due to the ease with which complete samples may be constructed and this, together with the simple forms of radio spectra, has allowed rather detailed evolution models to be derived (see Peacock & Gull 1981 and references therein).

Studies of this sort must assume a relation between luminosity, redshift and flux density, which is invariably taken to be that of an isotropic Friedmann universe. However, the recent discovery of the double and triple quasars has suggested that this neglect of gravitational lensing effects may be unjustified. Turner (1980) has suggested that two such extreme examples as 0957 + 56 and 1115 + 08 would not have been expected unless a large fraction of observed quasars were significantly affected by lensing. He goes on to show from an illustrative model that gravitational lensing could lead to apparent strong cosmological evolution

without any real effect being present. The purpose of the present paper is to investigate this suggestion in more detail, and in particular to examine the implications for the detailed models of radio-source evolution.

We shall attempt to derive the effects of lensing from first principles, using simple models for the individual lenses and for the lens population. Section 2 discusses the qualitative effects of lensing on cosmological data, and Section 3 presents a model for calculating the practical importance of the effect. The results of these calculations are given in Section 4, and possible resulting modifications to evolution models are discussed in Section 5.

A Hubble constant of $50 \, \mathrm{km \, s^{-1} \, Mpc^{-1}}$ will be assumed throughout this paper. The effects of uncertainties in this and other assumptions are discussed in Section 4.2.

2 The effects of lensing

2.1 GENERAL POINTS

It has long been recognized that distant objects may have their images distorted by the bending of light in the gravitational field of an intervening mass, leading to multiple imaging and considerable flux amplification. This possibility was first discussed in a cosmological context by Barnothy & Barnothy (1968), who suggested that all quasars were merely amplified Seyfert nuclei. Detailed calculations, however (e.g. da Silva 1970), indicated that only a tiny fraction of all observed quasars could be produced in this way, and the effects of lensing were dismissed as negligible in cosmological studies. There matters rested until Turner (1980) realized that, even if the intrinsic probability of a lensing event was small, selection effects would tend to favour those sources which had been amplified by large factors. However, Turner made no attempt to calculate the selection effects that would apply in practice, which is the problem we shall tackle here.

The first step in such a calculation is to specify the lenses to be considered. Any inhomogeneity can cause lensing effects, but we shall restrict ourselves initially only to galaxies and groups/clusters of galaxies (more exotic lenses will be dealt with in Section 5). For such objects, it is clear that there are no simple arguments which can eliminate the possibility that most radio sources might be significantly affected by lensing: for distributed masses, large amplifications can be caused without creating multiple images (see Section 3.2); furthermore, for all but the most massive lenses, any image splitting could be < 1 arcsec and so not readily observable. Also, the difficulty in detecting the lenses in the case of the double and triple quasars amply demonstrates that lensing galaxies (expecially if of low mass) could well escape detection in most cases. Finally, the common supposition that radio sources are immune to lensing on account of their extended structure need not be correct: many powerful sources (compact or classical double) contain most of their emission in structure of scale $\lesssim 1 \, \mathrm{kpc}$, which can be affected by lensing (see Section 4).

2.2 THE DISTRIBUTION OF AMPLIFICATIONS

The most important aspect of lensing is that it is a statistical problem. In a homogeneous Universe, the luminosity and redshift of a source determine its flux density uniquely; lensing means that, depending on the exact line of sight considered, a given source will generate a distribution of flux densities. We shall analyse this in terms of the distribution $F(A)$ of amplification factors, A, relative to a homogeneous Universe, in which the matter of all lenses is smoothed out. We may expect $F(A)$ to have the following qualitative features:

(a) $F(A)$ will be a skew distribution. If lensing is rare, then $F(A)$ will peak close to $A = 1$, but there will be a long 'tail' on the distribution towards high A — corresponding to occa-

sional close encounters with individual lenses. The form of this tail will depend both on redshift and on physical size of the object being lensed: generally, the amplitude of the tail will be larger at higher redshifts (probability of a lens along the line of sight increases) and for smaller sizes (effects of a given lens are stronger).

(b) In all cases, we know the mean value of A:

$$\langle A \rangle = 1 \tag{1}$$

This is surprising at first sight, since we tend to think of lensing as causing only amplification. However, consider the total flux of energy through any surface surrounding a given object: this is obviously independent of whether the matter inside that surface is distributed smoothly or in lumps. The mean flux density is therefore simply that expected in a homogeneous Universe in which the lens material is spread out uniformly. Thus, the mean amplification relative to a homogeneous Universe must be 1, simply through flux conservation, as pointed out by Weinberg (1976). The de-amplifications which are necessary to balance the amplifications from strong lensing events so that (1) is satisfied come about in two ways. Firstly, beams of light which avoid inhomogeneities are less strongly focused than in a homogeneous Universe of the same density, leading to some de-amplification relative to the homogeneous case (see Dyer & Roeder 1973 and references therein). Secondly, for those lines of sight which avoid a close encounter with a single lens, the beam of light is influenced weakly by many lenses. Rays of light can thus be caused either to diverge or to converge — leading to a scatter of amplifications. The relative importance of these two effects depends on the model of the Universe adopted, but in all cases they must combine so that the condition (1) is satisfied. This constraint of no mean amplification was violated by the models of Turner (1980) and, as we shall see in Section 5, strongly affects conclusions about the importance of lensing.

2.3 CALCULATING $F(A)$

Given (i) a model for the effects of an individual lens, and (ii) a model for the distribution of lenses in space, we can attempt to calculate $F(A)$ as follows:

For a source of a given size at a given redshift, we may integrate over all lenses and all space to find $N(>A)$ — the expected number of individual interactions leading to an amplification greater than A. Now, if $N \ll 1$, the probability of multiple lensing is negligible and we have

$$F(A) = \frac{dN(>A)}{dA}. \tag{2}$$

It is clear that this breaks down for small A: there is some critical amplification A^* for which $N(>A^*) = 1$, and multiple interactions are important in determining $F(A)$ for $A < A^*$. We shall not attempt to find $F(A)$ precisely below this limit. Instead, we note that the form of $F(A)$ should be determined approximately by the following arguments:

(1) $F(A)$ is given by equation (2) for $A \gg A^*$.

(2) For $A < A^*$, $F(A)$ must peak near to $A = 1$ with some spread of amplifications in such a way that the area under the distribution is 1 and the condition $\langle A \rangle = 1$ is satisfied. Although it is hard to find $F(A)$ exactly in this regime, it is clear that the scatter in amplification must be of order $A^* - 1$. With this assumption, plus the form of $F(A)$ for $A \gg A^*$ and the above conditions on $F(A)$, the behaviour of $F(A)$ for $A \simeq 1$ is reasonably well specified; since various of the observational parameters which determine $F(A)$ are uncertain, a precise calculation of $F(A)$ is not justified (see Section 4.2).

We now have a prescription whereby realistic forms for $F(A)$ may be found, given a knowledge of the lens population. This is considered in the next section.

3 The lens model

3.1 INDIVIDUAL LENSES

The effects of gravitational lensing by extended matter distributions have been treated by many authors, but for convenience we give here an outline of the theory (for details see Young *et al.* 1980 and references therein). Fig. 1 shows the lensing geometry for a spherically symmetric lens, in which case observer, lens, source and image all lie in the same plane. The angle α is the angle through which light is deflected, having passed within a distance b of the centre of the lens. The angles θ and ϕ are respectively the angle between the lens and the image, and the angle between the lens and the position of the source in the absence of lensing. D, D_1 and D_2 are 'angular diameter' distances which relate proper distance at a given redshift to angle (e.g. $b = D_1\theta$). Thus, for small angles, we have

$$\theta D = \phi D + \alpha D_2 \tag{3}$$

or

$$\alpha(b) \equiv \alpha(D_1\theta) = \frac{D}{D_2}(\theta - \phi). \tag{4}$$

In graphical terms, this is the intersection of a straight line with the curve representing the variation of bend angle with impact parameter. Since the bend angle must go to zero for large b, it is clear that the number of images must be odd (for non-singular mass distributions).

The important question for these calculations is what matter distributions are the relevant ones for galaxies and clusters of galaxies. Clearly, the exact distributions are complex, and we wish to find simplified models which nevertheless describe the lensing properties adequately. The simplest model which bears any relation to the real mass distributions in galaxies and clusters is that considered by Turner (1980): the singular isothermal sphere. This model has the density distribution of a self-gravitating, pressure-supported cloud: the projected surface density, σ, falls off with radius r as $1/r$. Density profiles of this kind are found in the outer parts of galactic systems, although there is a core in which the density rises less quickly than the $1/r$ law. We shall initially perform the lensing analysis for a zero core radius; the effects of this assumption are discussed in Section 3.2. For clusters of galaxies, the isothermal sphere with a variable core radius fits the distribution of galaxies very closely (see Bahcall 1977). For galaxies, the observed light distributions differ radically
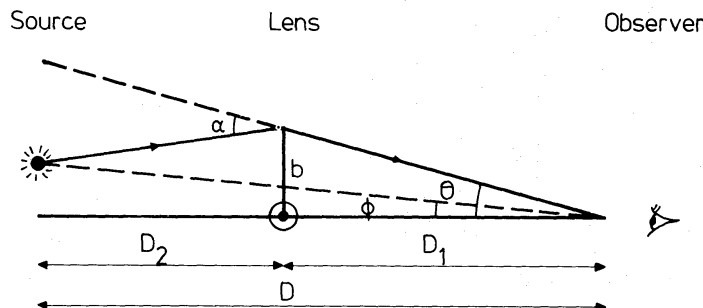
Figure 1. The geometry for a lensing event. The deflection angle α is a function of impact parameter b. θ and ϕ are the angles between the lens and respectively the image and the object. The distances D, D_1 and D_2 are in general the angular-diameter distances of cosmology.

from this model, especially for systems containing discs. However, for elliptical galaxies the outer envelopes often show a slow fall-off similar to the isothermal sphere (see Young *et al.* 1980). Also, for spiral systems, there is evidence in the form of flat rotation curves that much of the mass is not distributed in the same way as the light, but forms instead a 'heavy halo' (Ostriker, Peebles & Yahil 1974). The isothermal sphere model is thus in approximate agreement with our limited knowledge of the outer parts of galaxies and clusters of galaxies — which is where almost all lensing events will occur. This model also has the advantage of being something of an extreme: the divergence of the total mass implies that real matter distributions must fall off with radius more quickly than the model. Thus, the adoption of this model for the lenses should lead, if anything, to an over-estimate of the effect. Conversely, calculations which neglect the effects of galactic haloes run the risk of severely underestimating the importance of lensing. Given this particular model, we can show that the bend angle, α, is given by

$$\alpha = 4\pi \frac{\sigma_v^2}{c^2} \tag{5}$$

independent of radius, where σ_v is the line-of-sight velocity dispersion (see Young *et al.* 1980). The solution of equation (4) is now as shown in Fig. 2a; we have in general two images, for which

$$\theta = \phi \pm K, \tag{6}$$

where

$$K = \frac{4\pi\sigma_v^2 D_2}{c^2 D} \tag{7}$$

and the $\phi - K$ solution applies only if $\phi < K$. We are now in a position to calculate the image amplifications; these follow merely from the ratio of the areas of object and image, since
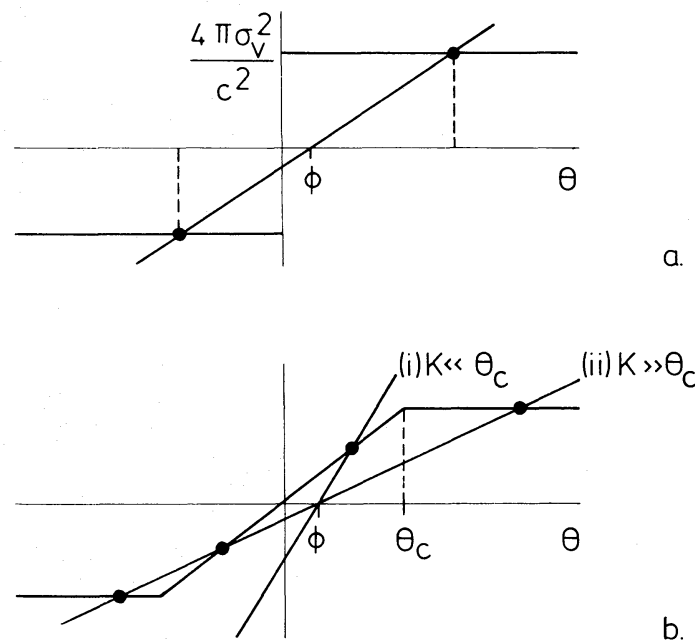
Figure 2. (a) The solution for images in the case of a singular isothermal sphere, for which α is a constant. (b) The solution for a non-zero core radius. Note that for $K < \theta_c$, $\theta \to 0$ as $\phi \to 0$ and large amplifications do not arise.

surface brightness is conserved by the gravitational field. For each image, this ratio is

$$A = \left| \frac{\theta}{\phi} \right| \left| \frac{d\theta}{d\phi} \right| \qquad (8)$$

provided the object has an angular size $\ll \phi$. Thus, we have

$$A = 1 + \frac{K}{\phi} \qquad (\phi > K) \qquad (9a)$$

$$A = \frac{2K}{\phi} \qquad (\phi < K) \qquad (9b)$$

for the total flux-density amplification. Since the model makes no claim to precise accuracy, we may combine these into the approximate form:

$$A = 1 + \frac{2K}{\phi}. \qquad (10)$$

In practice, infinite amplification is not achieved for $\phi = 0$ due to the non-zero angular size of the source. Consider a circular source of (unlensed) angular radius ψ, centred at $\phi = 0$. The amplification achieved in this case is

$$A = \left(1 + \frac{K}{\psi} \right)^2 \qquad (\psi > K), \qquad (11a)$$

$$A = \frac{4K}{\psi} \qquad (\psi < K), \qquad (11b)$$

which we approximate by

$$A = 1 + \frac{4K}{\psi}. \qquad (12)$$

Finally, for convenience we combine (10) and (12) to give a simple expression which interpolates between (10) for $\psi \ll \phi$ and (12) for $\psi \gg \phi$:

$$A = 1 + \frac{4K}{\psi} \left[1 - \exp \left(\frac{-\psi}{2\phi} \right) \right]. \qquad (13)$$

3.2 THE IMPORTANCE OF CORES

We must now consider the effects on this analysis of the existence in galaxies and clusters of 'cores' — central regions where the density stays relatively constant, causing the bend angle to drop within an angular radius θ_c. The image solution in this case is indicated schematically in Fig. 2(b), from which we see there are two main cases. Either $K > \theta_c$ and rays of light are bent around the core, leaving the amplification unaltered, or $K < \theta_c$, in which case we get approximately

$$\theta = \phi \Big/ \left(1 - \frac{K}{\theta_c} \right) \qquad (14)$$

and only one image. It is clear that in this case no very large amplifications are possible. In terms of the core radius, r_c, the condition for large amplifications becomes

$$r_c < \frac{4\pi\sigma_v^2}{c^2} \frac{D_1 D_2}{D}. \tag{15}$$

Even for high-redshift objects, $D_1 D_2/D$ can be no greater than about 500 Mpc, so the condition for the lens to be strong enough for effective amplification becomes

$$(r_c/\text{kpc}) \lesssim (\sigma_v/100\,\text{km s}^{-1})^2. \tag{16}$$

This condition is satisfied by galaxies (with typical cores of a few kpc and velocity dispersions of a few hundred km s^{-1}), but clusters (with typical cores of up to 1 Mpc and velocity dispersions of perhaps 1000–2000 km s^{-1}) are likely to be less effective lenses due to their lower degrees of central concentration.

We conclude that the strength of lensing amplification is closely related to multiple imaging; if the lens is incapable of generating a double image, it cannot cause large amplifications. Conversely, multiple imaging cannot occur without large amplification. Even with a zero core radius, we must have $A > 2$ for a double image. For a core near to the critical size, the threshold amplification will in practice be much larger. Hence, lensing events of large amplification need not be immediately detectable through multiple imaging.

3.3 THE LENS POPULATION

As with individual galaxies, the distribution of lenses is extremely complex — with both galaxies and clusters of galaxies exhibiting some degree of clustering which, together with their individual properties, must evolve with cosmic epoch. Fortunately, most of these complications may be neglected without seriously affecting our calculations.

The clustering of galaxies means that $F(A)$ will vary over different parts of the sky. However, for calculating the effects of lensing on all-sky samples we require the average $F(A)$, which is unaffected by clustering. Of course, deep surveys are carried out in small selected areas of sky, but these will usually be chosen to be free of obvious large clusters, so that lensing should be no more important in these than on average. A more difficult point is that galaxies tend to be associated with clusters of galaxies — i.e. that a lensing event involving a galaxy has a much higher chance of also involving a cluster (*cf.* Young *et al.* 1980, who find the effects of the cluster crucially important in modelling the double quasar). We shall neglect this problem and treat galaxies and clusters as though they were independent inhomogeneities. The assumption is that, while clusters can have a large effect on image structure and multiplicity, a given galaxy will not generally cause a greatly different total amplification merely because it lies in a cluster.

The evolution of lens properties with epoch is not well-determined, with known changes in colour and luminosity of galaxies relating more to changes in stellar populations than to the overall structure of the system. Fortunately, it is clear from equation (8) that lensing effects are less strong for lenses at similar distances to the object being lensed. Thus, even for quasars, the most important lenses lie at $z \simeq 0.5$ and we will not make significant errors in our calculations if we merely assume a constant comoving density of lenses whose properties do not change with epoch.

Our model now requires only the space density of galaxies and clusters as a function of velocity dispersion in order to make predictions. To achieve this, we follow Turner (1980) in noting that velocity dispersion correlates with optical luminosity, so that optical luminosity functions can be converted into distributions of lens strengths. The optical luminosity

function of galaxies has been investigated by many authors. The various determinations were compared by Felten (1977), who produced a compromise luminosity function of the following form:

$$dN = \phi^*(L/L^*)^{-5/4}\exp(-L/L^*)d(L/L^*) \tag{17}$$

where $\phi^* = 2.2 \times 10^{-3}\,\mathrm{Mpc}^{-3}$ and $L^* = 3.2 \times 10^{10}L_\odot$ and luminosities are calculated in terms of the $B(0)$ system (de Vaucouleurs & de Vaucouleurs 1964). The corresponding analysis for clusters and groups of galaxies was performed by Bahcall (1979) who found a similar form for the distribution of total luminosities of galactic systems (again in terms of $B(0)$):

$$dN = \phi_0(L/L_0)^{-2}\exp(-L/L_0)d(L/L_0), \tag{18}$$

where $\phi_0 = 1.6 \times 10^{-6}\,\mathrm{Mpc}^{-3}$ and $L_0 = 10^{13}L_\odot$. Unlike equation (17), (18) is unphysical in that it predicts an infinite luminosity density: Bahcall dealt with this problem by producing an all galaxy system (AGS) luminosity function which had the form (18) at high luminosities and (17) at low luminosities. For lensing purposes, we require something slightly different, since we must count each galaxy twice — once for itself and once for the group to which it belongs. In practice, this is not too hard since groups and individual galaxies segregate in luminosity: the contribution from (18) equals that from (17) at $L \simeq L^*$, the cut-off luminosity for the galaxy luminosity function. We may therefore combine (17) and (18) into an expression similar to Bahcall's AGS function:

$$dN = \phi_0 \frac{(L/L_0)^{-2}\exp(-L/L_0)}{[1+(L_0/2250L)]^{3/4}}d(L/L_0) \tag{19}$$

where ϕ_0 and L_0 are as in (18). Since we have seen in Section 3.2 that clusters may be less effective lenses than galaxies, we may consider (17) and (19) as possible alternatives for the luminosity function of lensing inhomogeneities.

Turner (1980) suggested that the conversion between luminosity, L, and velocity dispersion, σ_v, be performed in terms of the relation $L \propto \sigma_v^4$. This relation was found to apply for elliptical galaxies by Faber & Jackson (1976). Their result (based again on the $B(0)$ system) was

$$\frac{L}{L_\odot} = 6.8\,(\sigma_v/\mathrm{km\,s}^{-1})^4. \tag{20}$$

Although there is no reason to expect this to apply to clusters, a naive extrapolation to $L = 10^{13}L_\odot$ (the cut-off in equation 18) yields $\sigma_v = 1100\,\mathrm{km\,s}^{-1}$, which is a realistic velocity dispersion for a rich cluster. The relation (20) does seem, then, to have a general applicability to self-gravitating systems. The corresponding relation for spiral galaxies (i.e. between luminosity and 21-cm line width, V) was investigated by Aaronson, Huchra & Mould (1979) who found, working in the infrared H-band, a similar correlation

$$\frac{L}{L_\odot} = 1.2\,(V/\mathrm{km\,s}^{-1})^4 \tag{21}$$

obtained from data on the Virgo and Ursa Major clusters, assuming $H_0 = 50\,\mathrm{km\,s}^{-1}\mathrm{Mpc}^{-1}$. These workers also showed that a relation of this form arises quite naturally on dynamical grounds. However, in the optical, things are not so simple; Aaronson et al. (1979) found significantly flatter slopes for the $L-V$ relation in spirals when optical data were used.

Specifically, for the $B(0)$ system, their data on Ursa Major yielded a relation of the form

$$\frac{L}{L_\odot} = 250 \ (V/\text{km s}^{-1})^3. \tag{22}$$

This difference in slope was attributed to a variation of M/L_B with luminosity for spiral systems. At this point, we note that, in the isothermal sphere model, V is not the same as σ_V. For the isothermal sphere, we have

$$\rho = \frac{\sigma_V^2}{2\pi G r^2}, \tag{23}$$

where ρ = density and r = radius, from which it follows that the velocity, V, of material in a circular orbit is

$$V = \sqrt{2}\sigma_V \tag{24}$$

independent of radius. Now, the 21-cm line width is generally taken to measure $2V$, hence

$$V = 2\sqrt{2}\sigma_V. \tag{25}$$

Thus, in terms of the 'velocity dispersion' of spiral galaxies, (22) becomes

$$\frac{L}{L_\odot} = 5600 \ (\sigma_V/\text{km s}^{-1})^3. \tag{26}$$

To compare this with the result for ellipticals, note that (20) was established for σ_V in the region of $250 \, \text{km s}^{-1}$. For this, (20) and (26) yield values for $L/L_\odot$ of 2.66×10^{10} and 8.75×10^{10} respectively, which suggests that the lensing properties of the more luminous ellipticals and spirals are comparable.

Finally, therefore, we have the elements of our model. Equations (17) and (19) give two alternative luminosity functions, which may be converted into lens densities via either (20) or (26). Once the density is known, amplifications may be found from equation (13). By using various combinations of the above alternatives, we may hope to discover the uncertainties in our model predictions.

4 Results

4.1 PREDICTIONS OF $F(A)$

We can now apply the scheme outlined in Section 2.3 to calculate $F(A)$. Given the size and redshift, z, of the object to be lensed and the velocity dispersion and redshift, z', of a lens, we can calculate from (13) the impact parameter, b, corresponding to an amplification A. Hence

$$N(>A) = \int\!\!\int \pi[b(A,\sigma_V)]^2 (1+z')^3 dN(\sigma_V) d\tau, \tag{27}$$

where $d\tau$ is the element of proper distance

$$d\tau = \frac{c}{H_0} \frac{dz'}{(1+z')^2\sqrt{(1+2q_0 z')}}. \tag{28}$$

We note at this point that the distances D, D_1, D_2 in (13) should strictly be those derived by Dyer & Roeder (1973) for the inhomogeneous Universe. However, since these differ from

the homogeneous result by an amount less than that due to the uncertainty in q_0, we shall neglect this point and use the expressions for D, D_1, D_2 given by Young *et al.* (1980).

Before presenting numerical integrations of (27), we can predict many of the resulting features. Consider (13): for $A \gg 1$ and a point source, we have (putting $b = D_1\phi$)

$$A = \frac{8\pi\sigma_v^2}{c^2} \frac{D_1 D_2}{D} \frac{1}{b}.$$

(29)

Thus, since $N(>A) \propto b^2$, we have $N(>A) \propto A^2$ and $F(A) \propto A^3$. Therefore, we must have

$$F(A) \propto \frac{1}{A^3} \int_0^z \frac{D_1^2 D_2^2}{D^2} \frac{(1+z')}{\sqrt{(1+2q_0 z')}} dz'$$

(30)

and we need only find the constant of proportionality. Also, for a source of physical radius d, there is a maximum amplification A_{max}, given by (remembering $d = D\psi$)

$$A_{max} \propto \frac{\sigma_v^2 D_2}{d}.$$

(31)

And, since the maximum possible value of D_2 is D, we have

$$A_{max} \propto \frac{D}{d}.$$

(32)

Both (30) and (32) must stand independent of different assumptions about the lens population.

We now present results for numerical evaluation of $dN(A)$; we shall concentrate on a 'standard' model using galaxies and the $L \propto \sigma_v^4$ correlation (i.e. equations 17 and 20) and consider variations due to different assumptions later. Fig. 3 shows $dN(A)$ evaluated for objects with a range of physical sizes at a redshift of 1. We see the predicted $1/A^3$ law, steepening for A near to 1, with a cut-off which depends on physical size. For large A, these curves are well represented by

$$F(A) = \frac{a}{A^3} \exp(-A/A_{max})$$

(33)

with the 'tail amplitude' a independent of physical size. Fig. 4 illustrates the change of tail amplitude with redshift; as required by (30), $a \propto z^3$ for low redshifts, but the relation flattens to $a \propto z$ for $z \simeq 1$. From these numerical calculations we can find the constants in (30) and (32) and obtain the following expressions for the terms a and A_{max} in (33):

$$a = 1.5 \int_0^z \frac{D_1^2 D_2^2}{D^2} \frac{(1+z')}{\sqrt{(1+2q_0 z')}} dz',$$

(34)

$$A_{max} = 70 \, (DH_0/c)(d/\text{kpc})^{-1}.$$

(35)

Representative values for $d = 1$ kpc at $z = 1$ are $a = 0.02$, $A_{max} = 25$.

Finally, we consider the spread in $F(A)$ caused by multiple interactions. The numerical evaluations of $N(>A)$ can be used to find A^* (at which $N(> A) = 1$); as discussed in Section 2.3, we expect $A^* - 1$ to be a measure of the scatter of A about 1. The variations of $A^* - 1$
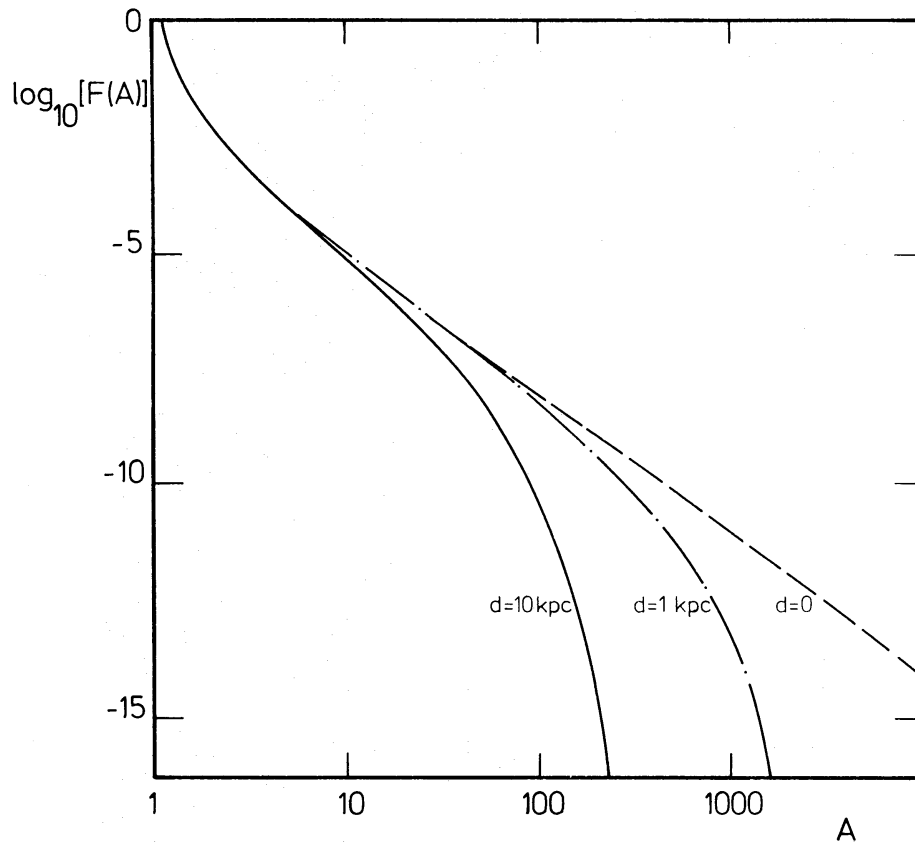
Figure 3. The function $dN(A)$ on a log-log plot. This has been evaluated at $z = 1$ for sources of linear size 1 and 10 kpc. Note the $1/A^3$ form at moderate A and (i) the steepening for $A \cong 1$ and (ii) the cut-off at high A.
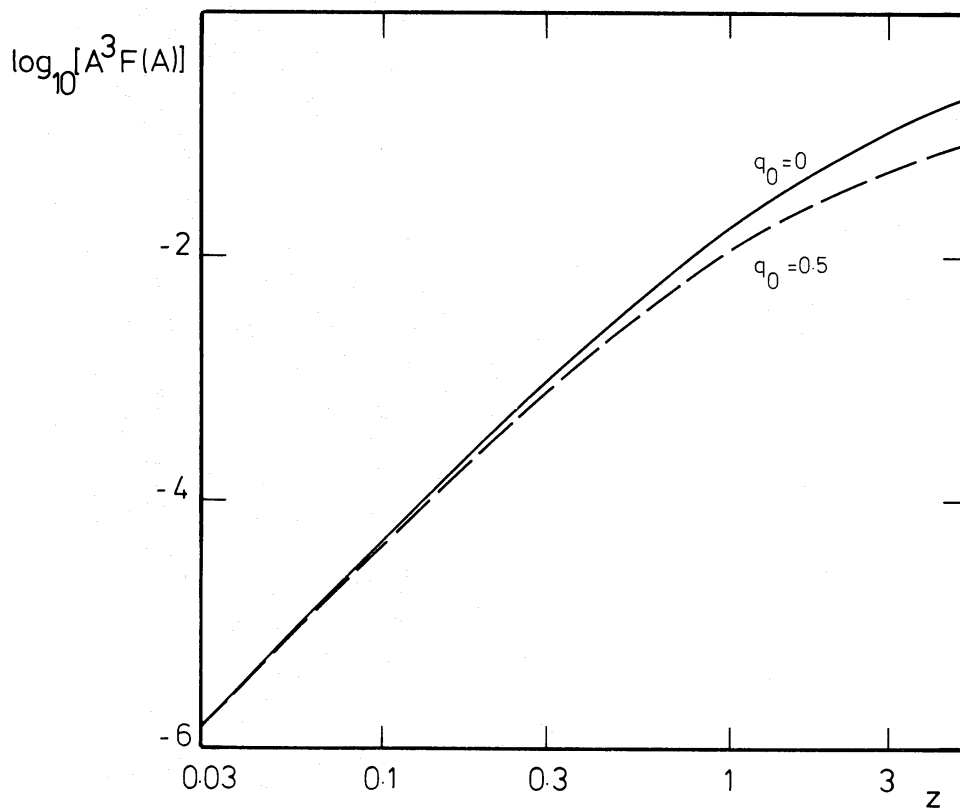
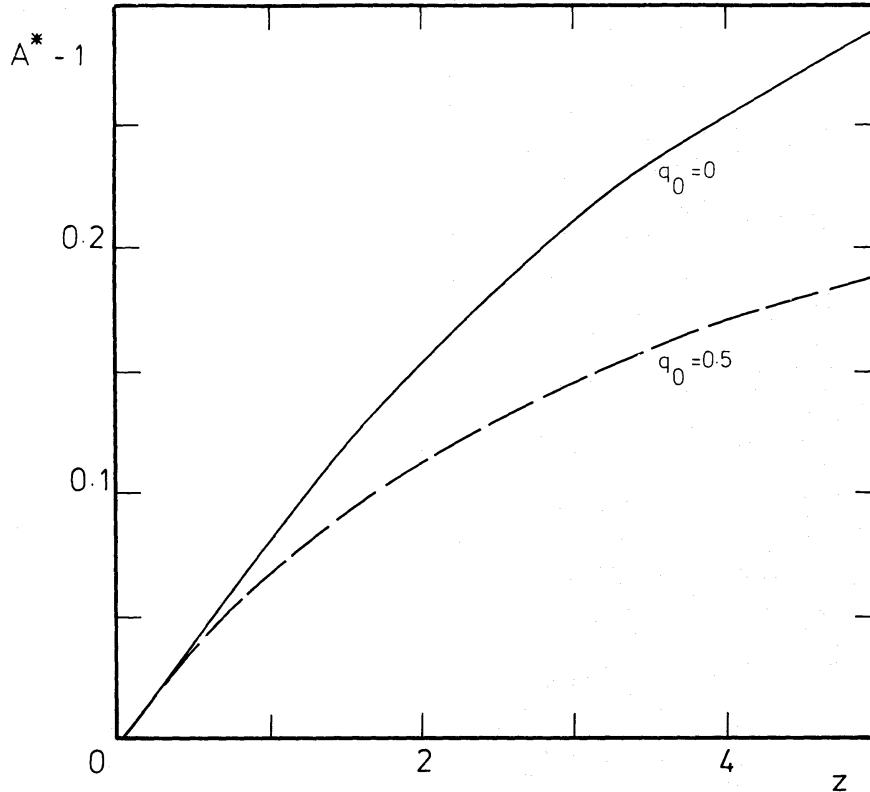**Figure 4.** The tail amplitude $(a = A^3 F(A))$ as a function of redshift.

Figure 5. The quantity A^*-1 (essentially the spread in amplification factors) as a function of redshift.

with z is shown in Fig. 5; the behaviour may be approximated by

$$A^*-1 = \frac{z}{12} - \frac{z^2}{225} \quad (q_0 = 0) \tag{36a}$$

$$A^*-1 = \frac{z}{12} - \frac{z^2}{80} \quad (q_0 = 0.5) \tag{36b}$$

independent of physical size.

We may now synthesize forms for $F(A)$ taking the tail as given by (33) and causing it to turn over on a scale of $A^* - 1$ such that the constraints $\int F(A)\,dA = 1$ and $\int A\,F(A)\,dA = 1$ are satisfied (the procedure used to perform this in practice is discussed in Appendix I). Some of the resulting forms for $F(A)$ are shown in Fig. 6: note how the spread and skewness (illustrated well in the log-log plot of Fig. 6b) increase with redshift.

4.2 UNCERTAINTIES IN $F(A)$

We must now consider the extent to which the above results are uncertain, due to inaccuracies in the assumptions made. The most basic uncertainty is that entailed by the adoption of the isothermal sphere model for the lenses; however, we have already argued that this should lead if anything to an upper limit on the size of the effect. Certainly, results such as the $1/A^3$ form of $F(A)$ do not depend on this model: for small ϕ (intrinsic angular separation of lens and source), the lensing amplification will go as $A \propto 1/\phi$ for any lens model, and it is this which leads to the $1/A^3$ form.

The numerical results of (34), (35) and (36) depend on the optical luminosity function adopted — (17) or (19) — and the form of the $L - \sigma_v$ relation used — (20) or (26). This was
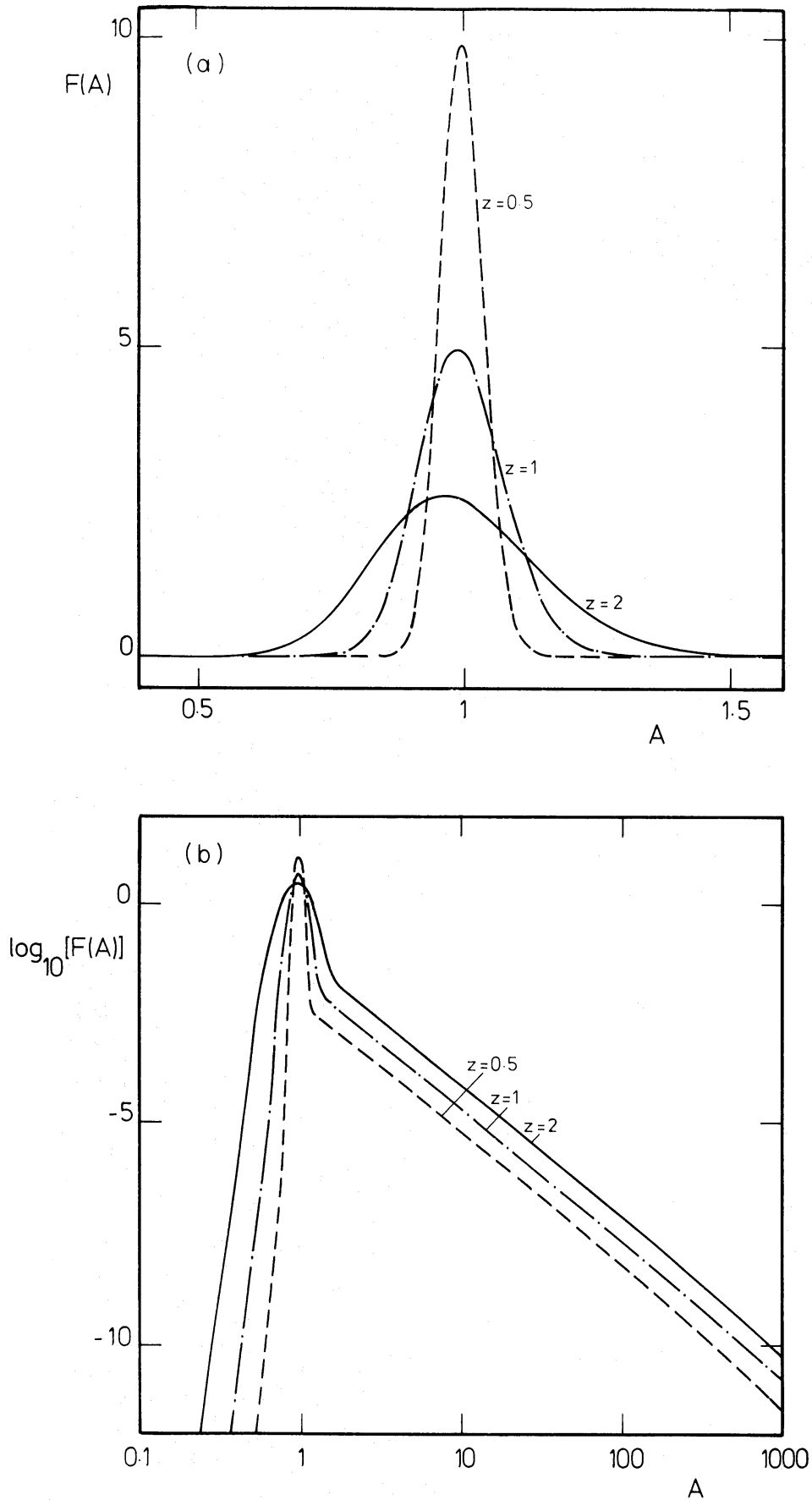
Figure 6. (a) Synthesized forms of $F(A)$ for a 10-pc source at redshifts of 0.5, 1 and 2. Note the increase of spread and skewness with redshift. (b) The same as in Fig. 6(a) but on a log-log plot to illustrate the power-law tail.

investigated directly by finding $N(>A)$ for different combinations of the various assumptions. Also, it has been suggested (Gott & Turner 1976) that the slope of the galaxy luminosity function at low luminosities is -1, not $-5/4$ as in (17). While this possibility is rejected by Felten (1977), the difference this would make in lensing calculations was also considered. The results of these calculations were as follows: the tail amplitude, a, and $A^* - 1$ were found to be uncertain by a factor of about 2. When galaxies alone were considered, our standard model of the luminosity function (17) and the $L \propto \sigma_v^4$ relation (20) gave the largest values of a and $A^* - 1$, whereas the luminosity function of Gott & Turner (1976) combined with the $L \propto \sigma_v^3$ law of (26) yielded the lowest results — approximately a factor of 2 smaller. Conversely, the addition of clusters via the AGS function (19) yielded values of a and $A^* - 1$ twice as large as the standard model.

The parameter A_{max}, on the other hand, was not so well determined. A_{max} really depends on the most massive lens present, i.e. on the maximum value of σ_v^2. Since this is a factor of 10 higher for clusters than for galaxies, it is clear that A_{max} is highly uncertain. We shall therefore generally assume $A_{max} = \infty$ in most calculations; but note that, even in the most favourable case, A_{max} for high-redshift steep-spectrum sources cannot be much greater than ~ 250 (the value for $d = 1$ kpc at $z = 1$).

Finally, there is the point that all our calculations have used $H_0 = 50$ km s^{-1} Mpc^{-1}. To see how this matters, consider equation (27) for $N(>A)$: the distances b and $d\tau$ are each proportional to H_0^{-1}. The density $dN(\sigma_v)$ is generated from a luminosity function such as (17) and a $L-\sigma_v$ law such as (20). In (17) the normalization constant ϕ^* scales as H_0^3 while L^* scales as H_0^{-2}; however, L^* is eliminated in terms of H_0–independent σ_v, so that $dN(\sigma_v)$ has only a simple H_0^3 scaling. Thus, in (27), all H_0 dependence cancels out. This is reasonable, since the argument depends only on distance-independent quantities such as σ_v and the angle ϕ.

We therefore conclude that the upper limit to $dN(>A)$ represented by our standard model can be too small by at most a factor of 2: further, this is possible only by assuming clusters to be centrally condensed to an unrealistic degree (see Section 3.2).

5 Evolutionary implications

5.1 RADIO–SOURCE EVOLUTION

All evolutionary statements are based on the redshift dependence of the radio luminosity function (RLF), but the RLF we deduce from observational data is now the true RLF convolved with the appropriate $F(A)$ for varying redshift and type of source. If alterations to the RLF are small, then we may adopt a perturbation approach and find the lensing correction by convolving $F(A)$ with the RLF inferred in the standard manner (if the effects are large then the problem is impossible, since we can never know $F(A)$ well enough to do the deconvolution properly). One problem with this approach is that observational data do not define the RLF uniquely (see Peacock & Gull 1981), and it is better to work with observed quantities such as the redshift-dependent source counts $dN(S, z)$. The redshift distributions are of course unknown at low flux densities (hence the uncertainty in the RLF), but most evolutionary conclusions are inferred from bright samples, and it is of particular interest to see how these are affected by lensing.

The possible effects on $dN(S, z)$ of convolution with $F(A)$ may be looked at in two ways: since the tail amplitude is generally small, we may be tempted to neglect this feature of $F(A)$ altogether and consider only the effects of smoothing $dN(S, z)$ with a quasi-Gaussian distribution whose width is specified by (36). However, if the source counts are

sufficiently steep, then the great excess of faint sources could make the tail important. Our investigation must therefore contain the following elements:

(i) Consider whether selection effects could raise the importance of the tail so that observed samples are corrupted by significant numbers of highly amplified sources.

(ii) If the tail is unimportant, what are the effects of smoothing $dN(S, z)$?

We note that any suggested alteration of evolution depends entirely on the extent of any changes made to $dN(S, z)$. This is quite important: even if most sources have been significantly lensed, this need not affect our statistical conclusions, provided we end up with the correct number of objects in a given flux density-redshift bin. As a preliminary, consider the effects of $F(A)$ on a differential source count of power-law form, $dN \propto S^{-\beta}$. It is easy to show that the resulting count has the same slope and an amplitude changed by a factor x, where

$$x = \int F(A)A^{\beta-1}dA, \tag{37}$$

so that, for $\beta = 1$ or 2, dN is quite unchanged, whatever $F(A)$. In practice, counts of power-law form over many orders of magnitude of flux density do not occur, but it is clear from (37) that the importance of the lensing tail is determined by the average slope of the counts: if the effective β is 4 or greater, then the numbers of faint sources rise more quickly than the $1/A^3$ probability of obtaining a large amplification falls. If slopes of this order are maintained over even 1 or 2 mag of flux density, then observed samples could be severely corrupted by highly amplified objects. However, such conditions are not encountered; the steepest source count known is for 3CR quasars, for which $\beta = 3.2 \pm 0.5$ (Laing *et al.* 1978). Furthermore, this and all other counts converge within one or two orders of magnitude of flux density to slopes of $\beta \simeq 1.5$ (e.g. Pearson & Kus 1978). It therefore seems that neglect of the lensing tail may be justified. To examine this for some practical cases, we use model 1 of Peacock & Gull (1981) to predict the counts of steep-spectrum and flat-spectrum sources for the redshift ranges $0.5 < z < 1$ and $1 < z < 2.5$ (shown in Fig. 7). Similar counts are produced by other models: the predictions all agree at high flux densities, and the speed of convergence to low flux densities is all that is uncertain.

We adopt average tail amplitudes for these redshift ranges of 0.01 and 0.04 respectively (see Fig. 4), implying intrinsic probabilities of $A > 2$ of 0.00125 and 0.005 respectively. We can now convolve these counts with the appropriate $F(A)$ to find the numbers of objects with $A > 2$ which would be generated by lensing. Since the maximum amplification is rather poorly determined (see Section 4.2), we shall assume for now that there is no limit to A for sources of either spectral type. The results of this exercise are shown in Fig. 8; this displays the ratio by which lensing due to the tail increases the numbers of objects in flux density-limited samples. While the difference caused by lensing is generally small (especially for the lower redshift range), the effects are uncomfortably large for high-redshift sources at flux densities above ~ 1 Jy, with 10–20 per cent of the observed samples consisting of highly lensed objects. The significance of these results, however, depends on the sample sizes available at such flux densities. The number of bright high-redshift objects that exist even over the whole sky is severely limited, and simple Poisson noise limits the precision with which source counts, etc., may be defined. The criterion for significant contamination due to lensing is therefore that the number of lensed sources must exceed the statistical fluctuations expected in limited samples. We can use the counts from Fig. 7 to generate the number N of sources with $S > S_0$ in a given area of sky. Now, using Fig. 8, we can predict the area of sky which must be observed in order for the number of lensed sources to be $\sqrt{N}$ (i.e. a 1σ
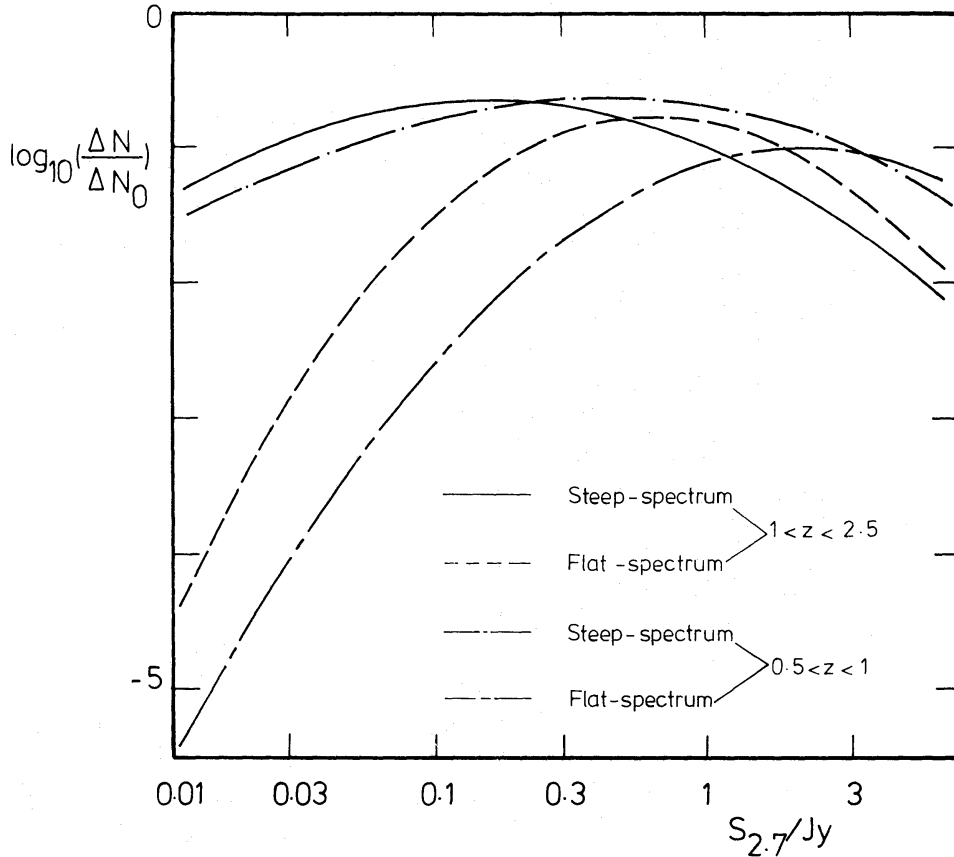
Figure 7. The differential source counts for steep-spectrum and flat-spectrum sources in the redshift ranges $0.5 < z < 1$ and $1 < z < 2.5$, as predicted by model 1 of Peacock & Gull (1981). The counts are normalized to the Euclidean form $N_0 (>S) = 100 S^{-1.5} \, sr^{-1}$.

detection of lensing). In all cases but for high-redshift steep-spectrum sources, this area is considerably in excess of $10 \, sr$ at all flux densities, implying that highly lensed objects never affect $dN(S,z)$ significantly. For the high-redshift steep-spectrum sources, the area falls below $10 \, sr$ for flux densities less than about $1 \, Jy$. However, the fall is slow and the area required to 'detect' lensing is still $2 \, sr$ at the lowest flux densities. Furthermore, for this class of object, our neglect of a maximum amplification is certainly incorrect and the curve shown in Fig. 8 must be a considerable over-estimate of the effect. Thus, even the marginal possibility of detecting gravitational lensing through all-sky surveys below $S_{2.7} = 1 \, Jy$ is unrealistic, and we conclude that the effects of the tail on $F(A)$ may be neglected. Finally, we note from Fig. 8 that the proportion of lensing contamination rises rapidly with flux density above $\sim 1 \, Jy$ (due to the steepness of the counts). Thus, with high-redshift objects at high flux densities standing the best chance of being highly lensed objects, we confirm Turner's (1980) conclusion that the most luminous objects known may be good candidates for lensing events.

We are now left to consider the effects of convolving the counts in Fig. 8 with $F(A)$ distributions which are quasi-Gaussian with mean 1. This is a far cry from the situation envisaged by Turner (1980), who neglected the condition $\langle A \rangle = 1$ and thus over-estimated the effects that lensing by small factors could cause. Avni (1981) amended Turner's illustrative model to correct for this, although his analogue of $F(A)$ consisted of 3 delta functions separated by a factor of 3 or greater in A. This is to be contrasted with our forms for $F(A)$, in which the spread is generally much smaller: for the two redshift ranges considered above, we have $A^*-1 = 0.06$ and 0.1 respectively. The effects of convolving the counts from Fig. 7
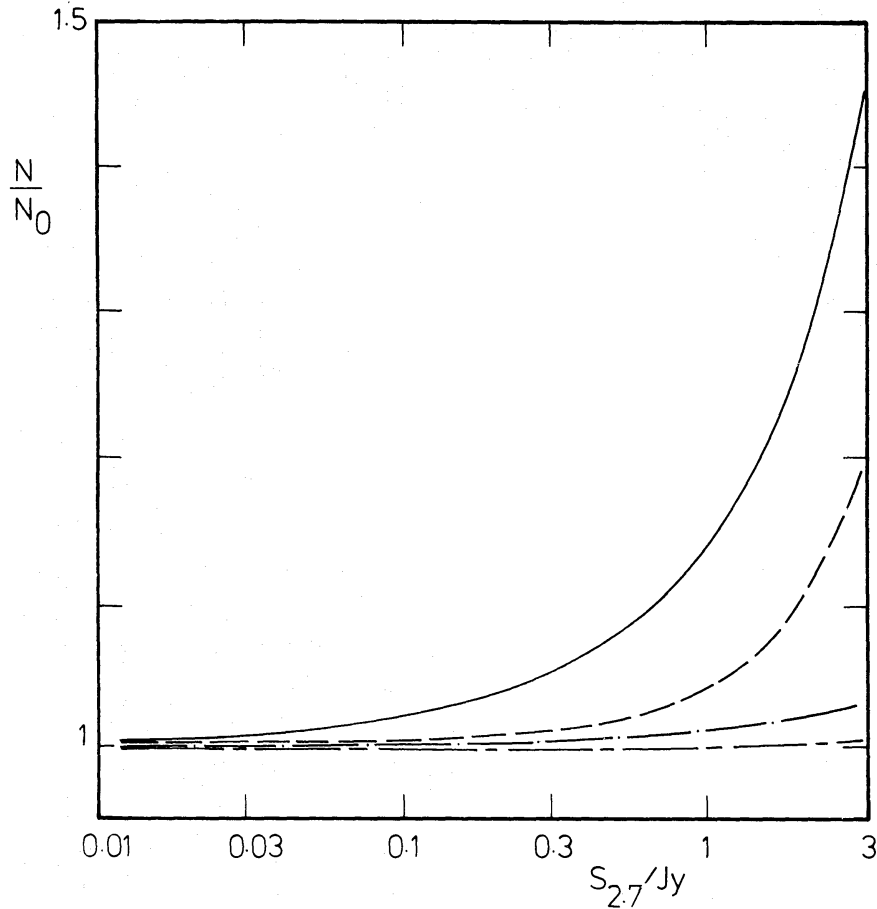
Figure 8. The effect of the $A > 2$ tail from $F(A)$ on the counts from Fig. 7. This figure shows the ratio of the *integral* source counts with the addition of lensed objects to the unperturbed counts. The key to the lines is the same as in Fig. 7.

with an $F(A)$ which is Gaussian with the appropriate width are shown in Fig. 9. This gives the ratio of $N(>S, z)$ after convolution with $F(A)$ to the initial value. Comparison with Fig. 8 shows that the changes are generally much smaller than those due to the tail on $F(A)$, so again there will be no significant change to the counts or to our cosmological interpretation of them.

5.2 QSO EVOLUTION

The above arguments concerning evolution of radio sources are equally applicable to samples of optically selected quasars and the evolution inferred from them. However, we must now consider a possible exception to the analysis presented so far, and ask whether any objects other than galaxies and clusters of galaxies could act as gravitational lenses. This question is particularly important for optical samples, since the optical source in quasars is so much smaller than the radio. Typical length-scales are $\sim 10^{-3}$ pc for the optical continuum source (from variability arguments) as compared to radio length-scales of ~ 10 pc for flat-spectrum radio cores (from self-absorption arguments). Hence, objects of much smaller mass may act as lenses in the optical case. It is possible to show that, for point mass lenses, the minimum mass which can lens an object of size d is (see Appendix II)

$$\frac{M_{min}}{M_\odot} \simeq 200 \frac{(d/\text{pc})^2}{(H_0/c)D}.$$
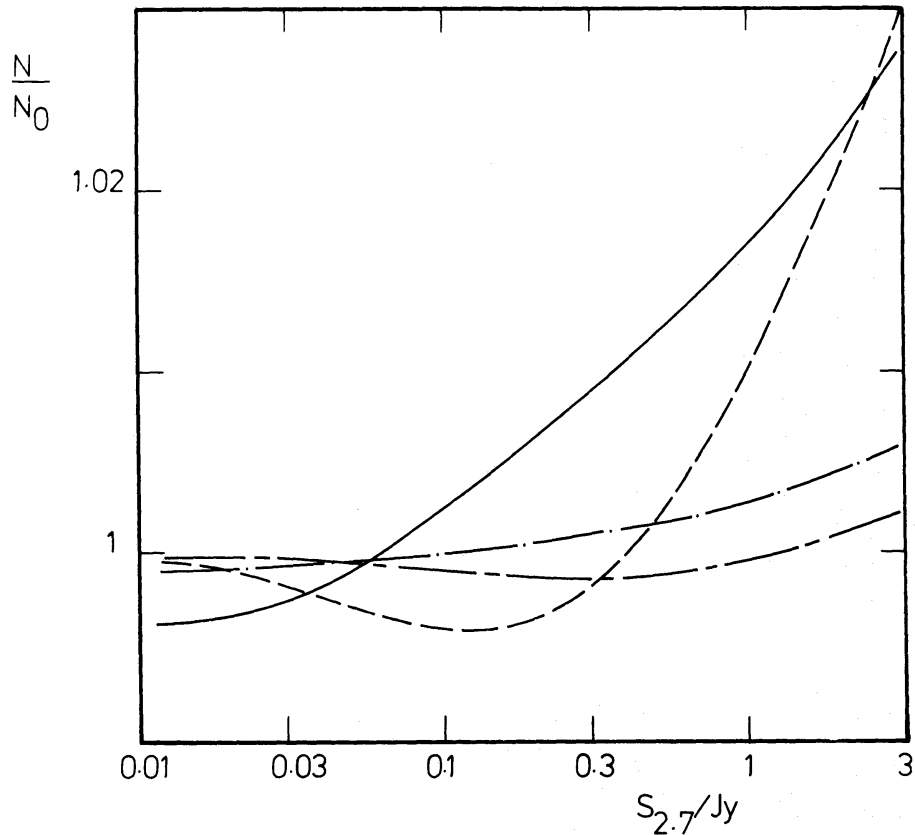
(38)

Figure 9. The effect on integral source counts of convolving with a Gaussian $F(A)$ with spread 0.06 and 0.1 for $0.5 < z < 1$ and $1 < z < 2.5$ respectively. The key to the lines is the same as in Fig. 7.

Thus, for the length-scales discussed above, the critical masses are respectively $\sim 10^{-4} M_\odot$ and $\sim 10^5 M_\odot$ respectively. The effects of lensing by a cosmological population of condensed objects were considered by Press & Gunn (1973). They found that a high-redshift object would be split into a roughly equal double by lenses of mass M, with a separation of about $2.6 \times 10^{-6} (M/M_\odot)^{1/2}$ arcsec. They further noted that such splitting (together with strong amplification) occurred with a probability $\sim \Omega_0$, independent of the distribution of M. Thus, if the 'missing mass' of the Universe is placed in such condensed objects, lensing could still be important. For lenses massive enough to affect radio sources there is a difficulty in making the objects dark enough (M/L of several hundred solar units). Further, the image doublings are predicted to be on the scales of m.arcsec or above, inconsistent with observed VLBI structures. For ultralow-mass stars, on the other hand, high M/L ratios and unobservably small splittings arise quite naturally. If the dark material of the Universe is of this form, then samples of optically selected quasars could be strongly affected by lensing, even for $\Omega_0 \simeq 0.1$. If this were the case, it would help explain the high ratio of radio-quiet to radio-loud quasars. Furthermore, this could provide an explanation of the difference in X-ray properties between the two classes of quasar: we know that the ratio of X-ray to optical luminosity for optically selected quasars decreases for the fainter quasars (Kembhavi & Fabian 1981). Thus, if most apparently bright optically selected quasars were intrinsically faint lensed objects, they would have a lower L_X/L_{OPT} than unlensed radio-selected quasars. It would of course be naive in the extreme to hope that all radio-quiet quasars could be accounted for in this way, but in seeking an explanation, this is one possible contributing effect.

6 Summary

This paper has presented an investigation of the practical importance of gravitational lensing in corrupting statistical studies of cosmological evolution.

Models of the lens population based on empirical luminosity functions and dynamical properties of galaxies and galactic systems have been used to derive the distribution of lensing amplifications $F(A)$. The resulting effects on cosmological conclusions were found to be small because:

(i) The intrinsic probability of a strong lensing event is small, and the redshift-dependent source counts are not steep enough to cause strong lensing to dominate through selection effects.

(ii) Flux conservation implies that there is no mean net amplification. Weak lensing therefore causes de-amplification as often as amplification and the form of the redshift-dependent source counts $dN(S, z)$ is preserved.

The possible effects of lensing by low-mass objects are harder to quantify, due to our ignorance of the composition of dark matter in the Universe. Evidence from VLBI indicates that this is not important for masses large enough to affect radio sources ($\gtrsim 10^5 M_\odot$), but we cannot be certain that optically selected quasars are not affected. This possibility will always raise some doubt both over evolutionary studies of optical samples and over attempts to account for the relation between radio-loud and radio-quiet quasars.

Finally, there is the fascinating point that, although gravitational lensing does not affect cosmological conclusions based on radio samples, it would have done if either the radio luminosity function had been much steeper or if the number density of lensing galaxies had been much greater. In a sense, then, cosmologists must count themselves fortunate to live in a Universe in which the view to high redshifts is not distorted.

Acknowledgments

References

Aaronson, M., Huchra, J. & Mould, J., 1979. *Astrophys. J.*, **229**, 1.
Avni, Y., 1981. *Astrophys. J.*, **248**, L95.
Bahcall, N., 1977. *A. Rev. Astr. Astrophys.*, **15**, 505.
Bahcall, N., 1979. *Astrophys. J.*, **232**, 689.
Barnothy, J. M. & Barnothy, M. F., 1968. *Science*, **162**, 348.
da Silva, L. N. K., 1970. *Nature*, **228**, 1180.
de Vaucouleurs, G. & de Vaucouleurs, A., 1964. *Reference Catalogue of Bright Galaxies*, University of Texas Press, Austin.
Dyer, C. C. & Roeder, R. C. 1973. *Astrophys. J.*, **180**, L31.
Faber, S. M. & Jackson, R. E., 1976. *Astrophys. J.*, **204**, 668.
Felten, J. E., 1977. *Astr. J.*, **82**, 861.
Gott, J. R. & Turner, E. L., 1976. *Astrophys. J.*, **209**, 1.
Kembhavi, A. K. & Fabian, A. C., 1981. *Mon. Not. R. astr. Soc.*, **198**, 921.
Laing, R. A., Longair, M. S., Riley, J. M., Kibblewhite, E. J. & Gunn, J. E., 1978. *Mon. Not. R. astr. Soc.*, **184**, 149.
Ostriker, J. P., Peebles, P. J. E. & Yahil, A., 1974. *Astrophys. J.*, **193**, L1.
Peacock, J. A. & Gull, S. F., 1981. *Mon. Not. R. astr. Soc.*, **196**, 611.
Pearson, T. J. & Kus, A., 1978. *Mon. Not. R. astr. Soc.*, **182**, 273.

Press, W. H. & Gunn, J. E., 1973. *Astrophys. J.*, **185**, 397.
Turner, E. L., 1980. *Astrophys. J.*, **242**, L135.
Weinberg, S., 1976. *Astrophys. J.*, **208**, L1.
Young, P., Gunn, J. E., Kristian, J., Oke, J. B. & Westphal, J. A., 1980. *Astrophys. J.*, **241**, 507.

Appendix I: An analytic form for $F(A)$

For large A, we have

$$F(A) = \frac{a \exp(-A/A_{max})}{A^3}$$ (A1.1)

This must fail near $A = 1$ where we require $F(A)$ to turn over on a scale of (A^*-1). We must further satisfy the following conditions: (i) $\int F(A) dA = 1$, (ii) $\langle A \rangle = \int A F(A) dA = 1$, (iii) $F(A) = 0$ at $A = 0$. A suitable adaption of (A1.1) which turns over correctly and has $F(0) = 0$ is

$$F_1(A) = \frac{a \exp(-A/A_{max})}{A^3 + \exp[-(A-A^*)/A(A^*-1)]}.$$ (A1.2)

To complete the distribution, we add to this

$$F_2(A) = \frac{b}{\sqrt{2\pi}(A^*-1)} \exp\left(-\frac{[\ln(A/c)]^2}{2(A^*-1)^2}\right)$$ (A1.3)

and adjust the constants b and c so that conditions (i) and (ii) are satisfied.

Appendix II: Lensing by point masses

For a point mass M, the bend angle α is given as a function of impact parameter b by

$$\alpha = \frac{4GM}{c^2 b}.$$ (A2.1)

The lens equation (4) therefore reduces to

$$\theta^2 - \theta\phi = \frac{4GM}{c^2}\frac{D_2}{DD_1} \equiv k.$$ (A2.2)

Thus, for a circular source of radius ψ, we have (putting $\phi = \pm \psi$)

$$\theta = \frac{\sqrt{(\psi^2+4k)} \pm \psi}{2}.$$ (A2.3)

The maximum amplification is thus the ratio of the image areas

$$A_{max} = \frac{\theta_1^2 - \theta_2^2}{\psi^2} = \sqrt{[1 + (4k/\psi^2)]}.$$ (A2.4)

The minimum effective mass for a linear size d is therefore

$$M_{min} = \frac{c^2}{16G}\frac{D_1}{DD_2} d^2$$ (A2.5)

which reduces to (38).